

A control hardware based on a field programmable gate array for experiments in atomic physics

A. Bertoldi,¹ C.-H. Feng,¹ H. Eneriz Imaz,¹ M. Carey,^{1,2} D. S. Naik,¹ J. Junca,¹ X. Zou,¹ D. O. Sabulsky,¹ B. Canuel,¹ P. Bouyer,¹ and M. Prevedelli^{3, a)}

¹*LP2N, Laboratoire Photonique, Numérique et Nanosciences, Univ. Bordeaux-IOGS-CNRS:UMR 5298, F-33400 Talence, France*

²*School of Physics & Astronomy, University of Southampton, Highfield, Southampton SO17 1BJ, United Kingdom*

³*Dipartimento di Fisica e Astronomia, Università di Bologna, Via Bertini-Pichat 6/2, I-40126 Bologna, Italy*

(Dated: 19 November 2020)

Experiments in Atomic, Molecular, and Optical (AMO) physics require precise and accurate control of digital, analog, and radio frequency (RF) signals. We present a control hardware based on a field programmable gate array (FPGA) core which drives various modules via a simple interface bus. The system supports an operating frequency of 10 MHz and a memory depth of 8 M (2^{23}) instructions, both easily scalable. Successive experimental sequences can be stacked with no dead time and synchronized with external events at any instructions. Two or more units can be cascaded and synchronized to a common clock, a feature useful to operate large experimental setups in a modular way.

I. INTRODUCTION

Computer control of experiments is a common task of ever increasing complexity in physics. The implementation of long sequences of events where different instruments must execute commands at a given time is mandatory for all but the simplest experiments.

In the past, the number of computer controlled instruments was relatively small and the type of interfaces was often limited to GPIB and RS-232. It is now common to require the control of tens of instruments via USB, Ethernet, PXI, VXI, and others, in addition to the legacy interfaces mentioned above. The problem of computer control is aggravated by the need to make frequent changes both to the experimental sequence and the set of instruments; versatility and ease of programming are essential features. Moreover, both software and hardware obsolescence can play a role, since the lifetime of an experiment is typically longer than the time scale over which operating systems and computers' architectures evolve. From the software point of view, the problem has been tackled by developing libraries with a unified syntax for many interfaces¹ and complete frameworks^{2,3}, aimed mostly at large scale experiments in particle physics.

Here, we focus on the specific problem of controlling AMO experiments where usually outputs are limited to digital and analog signals changing according to a well defined temporal schedule. By “well defined” we mean that most operations must take place with a strict temporal resolution, typically of the order of 10 μ s or better for a cold atoms experimental setup. It is generally not possible to fulfil such a constraint with a modern general purpose multitasking operating system (OS), so dedicated OSs have been developed. Both commercial⁴ and open-source⁵ real-time operating systems (RTOS) are available. Reasonably complex AMO experiments⁶ have been controlled with the RTOS described

in Ref. 5. While the software approach has the advantage of simplicity, versatility and, in case of open-source solutions, low cost, a hardware one has generally superior performances in terms of temporal resolution. In the latter case it can actually be implemented a finite-state machine (FSM) synchronous with a common master clock (MC), where the digital outputs of the FSM, interpreted as commands by some auxiliary hardware modules, are sent out only at state transitions. The actual execution time of a command clearly depends on the modules response time, cable induced delays etc. Often, however, for a MC in the 1 MHz to 10 MHz range and typical AMO laboratory size experiments, these effects can be neglected, at least for digital signals, so delay and jitter are both a small fraction of the MC period. A possible implementation of the FSM mentioned above is a digital pattern generator (DPG), i.e. a device that stores in its internal memory a two-column matrix where the first column represents a time interval expressed in MC cycles while the second column gives the state that a sufficiently large number of digital outputs should assume at that transition time. Often, as in our case, it is more convenient to store not the absolute time but the interval from the previous transition to increase the maximum time span of a pattern.

Once the matrix is loaded into the DPG memory, execution can be started via a software command or an external hardware trigger. DPGs are commercially available⁷ or have been implemented in software in dedicated microprocessors running a single process i.e. a delay loop⁸. The abundance on the market of plug-in modules carrying a FPGA, plus a synchronous dynamic random access memory (SDRAM) chip, and some kind of fast interface, usually USB or Ethernet, gives the possibility of implementing high performance DPGs using a low-cost and easily available, credit-card size modules. Note that the most recent, high performance, FPGAs might be available on a module quite before they find their way into full featured commercial products.

A home-made DPG based on open-source software is more resilient, in our experience, to the main problem plaguing control hardware setups: obsolescence. Closed-source drivers for plug-in PC boards might not be updated for new OS versions after a few years; even the connectors used to fit the boards in

^{a)}Electronic mail: marco.prevedelli@unibo.it; The following article has been accepted by Review of Scientific Instruments. After it is published, it will be found at <https://publishing.aip.org/resources/librarians/products/journals/>.

the PC may disappear! The shelf life of a FPGA-based module is short, but given its limited cost, is very convenient to stockpile them while available. When, eventually, the module becomes obsolete, migrating to an updated version requires a relatively minor effort involving redesigning the printed circuit board (PCB) hosting the module and porting mostly open-source software and firmware.

DPGs can be used to drive directly the digital output lines of a control hardware as suggested in Ref. 8, but versatility can be added by connecting a DPG to a primitive digital bus with address and data sections. The DPG acts then as a master module and performs timed write operations on auxiliary modules implementing standard functions such as control of digital and analog outputs (DO and AO respectively) or RF signals (RFO). We define, for brevity, the combination of DPG and auxiliary modules operating synchronously with the MC as “synchronous control hardware” (SCH). A PC, possibly running a RTOS, usually takes care of the rest of the instruments, performing tasks that are not time-critical, using software timers.

This basic architecture has been adopted by many different groups in AMO physics and multiple designs have been published in literature ranging from specific applications⁹ to complete general purpose designs including both software and hardware descriptions.

These solutions allow control of complex AMO experiments developed for diverse research fields ranging from quantum metrology¹⁰, frequency standards¹¹, to quantum simulation¹².

Some recent articles published in this journal are, in chronological order, Refs. 13–19; together with references therein, they give a broad review on the subject. Moreover, various groups report online on their control systems^{20,21}. As we mentioned above, obsolescence is often the main limiting factor for these designs so, usually, any hardware that is maybe ten years old or more is using some outdated or hard to find components. For example, parts of the circuit described in Ref. 13 are implemented with obsolete medium scale integrated circuits, while the control systems described in Refs. 15, 20, and 21 employ PC plug-in and/or PXI cards not in production anymore.

We present here the SCH that we developed for cold atom experiments in atom interferometry²² and cavity QED with Bose-condensed gases²³, focusing specifically on our latest DPG, capable of storing up to $8 M = 2^{23}$ instructions (see 24), controlling up to 128 auxiliary modules and running with a MC of 10 MHz, which could also be used by itself, as a replacement for the design discussed in Ref. 8.

The main difference between our design and most of those recently published is essentially a simpler centralized architecture instead of a distributed one.

As an example, Refs. 17–19 share the same architecture implemented in Ref. 13, where every intelligent module (IM)²⁵, i.e. a module implementing a bidirectional fast communication interface, carrying a FPGA or a CPU, has a comparatively small first-in-first-out (FIFO) instruction buffer but communicates with the PC or other modules to receive data even when executing a sequence of instructions. In this way the maxi-

mum sequence length is not limited by the FIFO size.

Moreover, in order to strictly bound the worst case delay for arbitrary large systems, each module usually drives only a rather limited number of outputs, compared to our design. This allows arbitrary expansion of the control hardware without any increase in latency.

By comparison we take advantage of the large amount of SDRAM currently available and its large readout bandwidth to implement a centralized system with just one IM that will be sufficient to drive enough outputs to control most AMO experiments. This reduces the complexity of all the auxiliary modules, since none of them has to be an IM, without a serious loss of performance.

It should be mentioned that an intermediate solution has been also adopted^{14,15} by storing the columns of the DPG matrix in separate devices. A master module stores the first column, i.e. the temporal data, and sends a pseudoclock signal to the auxiliary modules. A pseudoclock has a positive edge transition synchronous to the MC only when any of the auxiliary modules must change its output. Each auxiliary module, in turn, stores its version of the second column of the DPG matrix, i.e. the output data, in an internal FIFO. An excellent discussion of the pros and cons of this approach can be found in Sec. III of Ref. 14.

In the following sections we describe in detail the architecture of the our SCH (Sec. II) and, specifically the DPG performance and the RFO modules (Sec. III). Finally in Sec. IV we discuss possible improvements.

In order to provide useful material both to those interested in a complete, out-of-the-box, control system and to those that would like to modify our work or to integrate parts of it into other available designs, we provide the complete system documentation²⁶ including hardware design files and full source code for the firmware and the software.

II. SYSTEM ARCHITECTURE

The SCH interfaces with any PC using a USB 2.0 connection and synthesizes digital, analog, and RF signals for the experimental setup, as shown in Fig. 1.

The master module stores the instructions received from the PC and, after receiving a software or a hardware trigger signal, executes timed write operations on the bus, thus implementing the synchronous component of the control hardware. The bus has a data width of 16 bits and an address width of 7 bits. The only control signal is a strobe line since a master write is the only allowed bus operation.

To our knowledge this bus was originally developed in Paris about 20 years ago²⁷, and is still in use at least as reported in Refs. 20 and 21.

Any auxiliary modules latch the content of data bus at the rising edge of the strobe signal when the content of the address bus matches the module’s address.

Due to the primitive nature of the bus, modules can not return data to the master. Hence, whenever data must be acquired, some specific hardware, e.g. a digital oscilloscope or an ADC sampling card, must be programmed by the PC via an

external interface before starting the program execution and triggered, when required, by the SCH. Finally, at the end of the experimental sequence, data must be acquired, processed and stored by the PC before starting the next sequence.

A similar approach, based on triggering dedicated external instruments, can also be used for generating complex waveforms when it is impossible or impractical to use a standard AO channel controlled by the SCH. In Fig. 1, a module implementing the last two functions is represented as the generic analog I/O box.

Presently, only one module at a time can be addressed, limiting the possibility of a simultaneous change of the output lines. A detailed discussion on this point together with a possible improvement is deferred to Sec. IV.

A. Master module

The plug-in FPGA module implementing the DPG in the SCH is the USB-FPGA module 2.04b from ZTEX²⁸. This module includes a Xilinx Spartan 6 FPGA, interfaced to USB 2.0 via a Cypress USB-FX2 microcontroller, and to a 64 Mbytes, double data rate (DDR) SDRAM chip via a 16 bits bus capable of running at 200 MHz. The module hosts a serial EEPROM to store the FPGA firmware.

The FPGA module is used to control the peripheral cards via a parallel and write-only bus. A series of write operations on the bus at specified time intervals can be downloaded in the board memory and later executed sending either a software command or a hardware trigger. We call each timed write operation an *instruction* and a series of instructions a *program*. The maximum size of a program is 8 M instructions, limited by the available SDRAM. For reference, a typical program length in our experiments is of the order of 10^4 instructions.

The module operates with a MC at 10 MHz, provided either from an external source or, for simplicity, synthesized from an onboard 24 MHz quartz of unspecified accuracy. Replacing the quartz with one of known specifications is a simple operation. Internally, the FPGA operates at $f_i = 200$ MHz. If f_c denotes the MC frequency a strobe pulse has a width of $1/2f_c$ and the temporal granularity of the SCH is $1/f_c$, i.e. 100 ns, which is adequate for most AMO experiments. On the other hand, the longest programmable interval between two instructions is $(2^{36} - 1)/f_c$, corresponding to about 6872 s. Longer intervals can be programmed by inserting “dummy” write operations i.e. instruction not followed by a strobe pulse. When using the external trigger, the input signal is sampled at f_i , to reduce the risk of missing short pulses, but execution will start at the next positive edge of the MC, as expected in a SCH.

Since an instruction is coded by 8 bytes in the module’s SDRAM, the required peak bandwidth between the SDRAM and the FPGA is 76.3 Mbytes/s at $f_c = 10$ MHz. This is more than a factor 10 smaller than the peak bandwidth of 800 Mbytes/s achievable with this module; increasing f_c up to at least 40 MHz should be therefore possible.

The program is loaded into the module memory through the USB 2.0 bridge and a parallel interface from the microcontroller and the FPGA, whose bandwidth is limited at a mea-

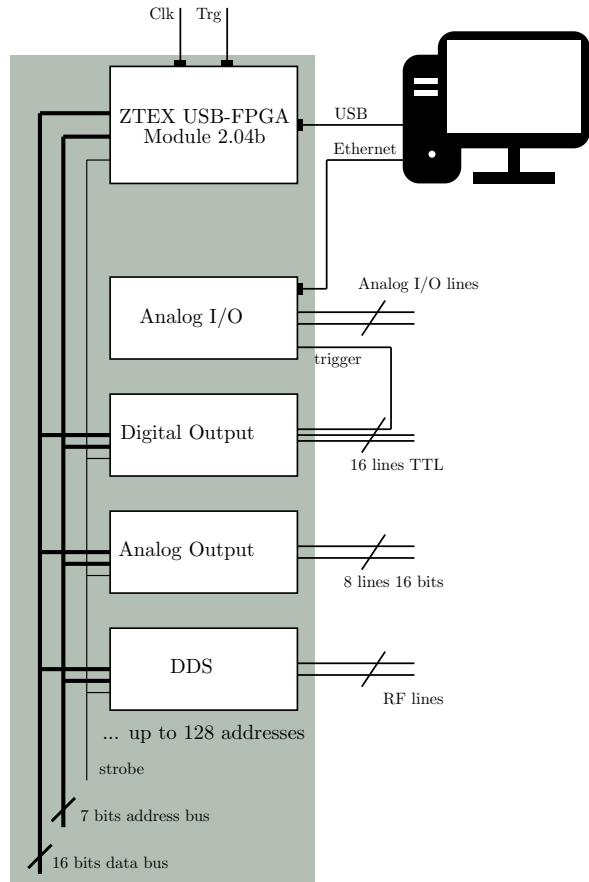


FIG. 1. Typical Architecture of the control hardware. The master controller is a FPGA card, connected to a PC via USB, driving modules via a digital bus. The system can be clocked internally or via an external signal connected on the “Clk” input; the program execution is controlled either via a software trigger from the PC or the “Trg” input. Up to 128 modules providing digital, analog, and RF outputs can be connected on the bus. The system can provide precise trigger signals to other hardware, here represented as a generic analog I/O unit, interfaced to the PC for programming and data acquisition.

sured average of about 5×10^5 instructions/s by the USB interface.

Break points can be inserted in a program after any instruction, in order to suspend execution with the output lines in a well determined state for debugging purposes or to wait for an external event. Program execution can be resumed with a digital signal or with a software command. This mode of operation can be exploited, for example, to synchronize the experiment with the power line, to reduce noise, and to monitor trap loading and trigger at a specified fluorescence level. A more complex SCH can be implemented by adding a cascade of ancillary master modules waiting for a trigger sent from an upper level in order to implement a tree structure similar to that described in Ref. 18. Clearly, in this case, an external common MC shared by all the modules should be used. This

will be discussed in more detail in Sec. IV.

B. Auxiliary modules

Many auxiliary modules have been developed but the most common ones are of three types: DO, AO, and DDS-based RFO. In addition to these modules, a general purpose analog I/O module for complex operations is often needed. Here we provide a quick overview of our most common modules even if they are not the main focus of this article; the target is to give an overview of all the hardware necessary for assembling a control hardware.

All the modules fit on 100 mm×160 mm Eurocard PCBs, to be mounted in 3U, 19" racks, and have their addresses programmed with miniature switches. The master module cannot read from the bus, so the software must have an *a priori* knowledge of auxiliary modules' addresses and functions. A more advanced, self-configuring design, can be implemented, if desired.

The DO modules are just an address decoder and a 16 bits latch so when writing to a DO module the content of the data bus is stored and transferred to its 16 output lines. All the lines on the same DO module can be changed simultaneously while changes on lines on different modules are separated by at least one MC period.

The AO modules are almost as simple, including a 16 bits DAC per address, generating an analog voltage, typically in the ± 10 V range. Parallel input DAC with the inputs connected to the data bus are particularly convenient and, in order to increase the number of outputs per PCB, we have recently developed an 8 channel, 16 bits DAC with parallel input, based on the Texas Instruments DAC8728. This AO module responds to 8 addresses, one for each channel. Again writing to different AO channels can not be simultaneous. The minimum delay of 1 MC period is however often negligible when compared with the typical settling time of a DAC chip. As an example the DAC8728 has a settling time to 1 LSB for a full range voltage step of about 15 μ s. We will discuss in Sec. IV possible schemes to overcome this limitation.

The RFO modules are based on DDS chips from Analog Devices. Different chips have been adopted over time, depending on specific applications. Our most commonly used chip has been the AD9958, which has two independent DDS channels clocked at 400 MHz and can generate RF signals up to 160 MHz with a frequency resolution of about 0.1 Hz. The output includes a 10 bit linear amplitude control. The maximum output power is +10 dBm.

For higher frequency and better resolution we have recently developed a module based on the AD9912 chip, a single channel DDS is capable of a maximum clock frequency of 1 GHz, producing a RF output up to 400 MHz with a resolution in the few μ Hz range. Amplitude control is provided by a programmable logarithmic attenuator with a dynamic range in excess of 30 dB in 0.25 dB steps (Analog Devices HMC759). The module output power is again at least +10 dBm.

We will refer in the following to the single channel and the dual channel modules as RFO1 and RFO2 respectively.

The RFO modules are the most complex modules and pose some challenges for inclusion in the SCH. For a precise arbitrary frequency ramp, some chips, i.e. the AD9954 or the AD9910, include an internal volatile memory where a table of arbitrary frequencies can be stored and later recalled automatically with a programmable delay between consecutive steps. The special case of a linear frequency or amplitude ramp is commonly implemented in hardware in many DDS chips, like the AD9958, so it is often sufficient to program the start and stop values, the step size and the dwell time at each point.

In both cases, however, a rather complex programming sequence is needed. Even a discrete frequency and amplitude step might require sending more than ten bytes to a DDS chip. Most chips have only a serial interface, so some logic is required to convert the 16 bits read from the data bus, decode them, and finally send the proper programming sequence to the DDS. This introduces a delay, between the moment when the command is issued and the one when the RF appears at the output, which can be large when compared with $1/f_c$. Moreover, 16 bits do not contain enough information to fully specify frequency and amplitude even for a single RF channel. There are two possible, simple solutions.

The first consists of assigning a separate address for frequency and amplitude for each RF channel and mapping, linearly, the values on the data bus to the frequency range actually required for a specific application. As an example, consider driving an acousto-optic modulator operating at its central frequency, in this case of $f_0 = 80$ MHz. The -3 dB bandwidth of the modulator is typically limited to $f_0 \pm 30$ MHz so the 2^{16} values on the data bus could specify, a frequency in the interval 50–110 MHz with a frequency resolution of the order of 1 kHz, which is adequate for most applications.

The second possibility is to use the content of the data bus as a pointer to a lookup table (LUT) stored in memory on the RFO module, where the complete state of a DDS driving RF channel is stored. The total number of combinations of frequency and amplitudes typically used in a given experimental sequence is a small fraction of all the possible values given the DDS resolution. This offers versatility at the cost of the increased complexity of generating and sharing the LUT tables between the modules and the PC.

In both cases, the module must include memory and processing capabilities. The two natural choices are a FPGA or a microcontroller. A FPGA will allow driving the DDS serial interface at a speed close to the maximum bandwidth, minimizing the output delay but with greater complexity and cost. A microcontroller, on the other hand, will provide a simple and cheap solution with a larger delay.

Our RFO modules include a microcontroller with USB interface (Microchip PIC 18F2550) and use the LUT model. The LUT is loaded and updated in the microcontroller's flash memory from the PC via USB. Both RFO modules share the same PCB hosting the microcontroller and the bus interface while the DDS and the other RF components are on a separate daughter-board. This modular structure simplifies the upgrades necessary when better DDS chips become available.

The typical delay between a write operation and the RF output change is of the order of a few tens of μ s, specifically 30

μs per channel when changing both frequency and amplitude with the RFO2 module and about $25 \mu\text{s}$ for the same operations for the RFO1 module.

When this sort of delay is not acceptable we can adopt a partial workaround: most DDS chips have double-buffered registers, meaning that the new frequency, amplitude etc. are preloaded in buffers and transferred to the DDS core only after pulsing a dedicated line. We usually have the microcontroller applying the pulse as soon as the data are sent, but we have the option to delay the pulse with a second write operation on the bus. This means that we can change the RF output synchronously with bus write operations as soon as we allow enough time, as specified above, between two consecutive state changes. Note that for the RFO1 module this method does not apply since the amplitude control is implemented with an external attenuator.

More advanced, albeit more complex, FPGA-based DDS designs have been published in Refs. 16 and 18.

Except for the "Trg" and "Clk" lines (see Fig. 1), this control hardware does not provide integrated input lines, either digital or analog, given the unidirectional nature of the system bus. The possibility to acquire signals is implemented with external hardware synchronized by DO lines: for example, the open-source STEMLab 125-14 module²⁹ can provide 2 inputs sampled at up to 125 MHz, with 50 MHz analogue bandwidth and 14 bit amplitude resolution, and auxiliary analogue inputs at 250 kHz with 12 bit resolution. The STEMLab board provides analog output lines with comparable bandwidth and resolution, and 16 general-purpose input/output (GPIO) lines. A STEMLab module can be triggered at the desired time by a DO line, while communication with the PC controlling the experiment uses a 1 Gbit/s Ethernet interface, as shown in Fig. 1. Typically this module provides the analog input (AI) function for i.e. sampling the fluorescence signal of a detection photodiode. The board can process, store and finally notify the PC that the data acquired are available. For convenience we have prepared a simple PCB hosting the STEMLab board to derive its supply and to be mounted in a 19" rack with the other modules.

C. Software

There are a few different software layers in a control system. In our experience, trying to use open-source or, at least, free software at every layer minimizes obsolescence and portability problems. Hardware and software are as independent as possible in this system, to allow for partial or incremental upgrades.

The firmware required by the auxiliary modules, notably the aforementioned RFO modules, includes the code for the microcontroller written in C and compiled with an open-source compiler for small devices, SDCC³⁰ and some simple Verilog code for a complex programmable logic device, (CPLD) that provides the interface to the bus. The LUT size, stored in the microcontroller flash memory, is 16 kbytes, sufficient for storing, for example, 2048 different combinations of amplitude and frequency for the RFO1 module or 1024 com-

binations of frequency, phase and amplitude for each channel of the RFO2 module.

We have actually developed two different firmware versions for the RFO2 module. The first one, simpler and sufficient for most applications, only sets phase, frequency and amplitude for each channel. The second takes full advantage of the chip's capabilities, allowing linear frequency (amplitude, phase) ramps and frequency-shift (amplitude-shift, phase-shift) keying modulation up to 16 different values.

For the RFO2 module, therefore, specifying values for the LUT is complex enough that we have chosen to implement a description based on the extensible markup language (XML) format, while for the RFO1 a simple text file with frequency-amplitude pairs is used.

The master module requires firmware for the FPGA and for the microcontroller controlling the USB interface.

The master module actually comes with an open-source default firmware for the microcontroller, implementing a high speed bridge from the USB to the FPGA that we found adequate for our purposes. The code can be easily modified and recompiled with SDCC if required.

The firmware for the FPGA is written in Verilog and compiled using the free version of the design software provided by Xilinx³¹. The code uses, whenever convenient, proprietary black-boxes that are freely available but not open-source. Specifically in this design we take advantage of the SDRAM controller and the FIFO generator. For a migration to full open-source code, we remark that the most complex module is the SDRAM controller and it could be replaced with designs from open-source repositories such as Ref. 32.

The Verilog code includes a main FSM (MFSM) that accepts and executes the commands sent to the FPGA and, finally, replies to the PC when appropriate, a memory interface and the MC-synchronous FSM (SFSM).

The commands follow a simple custom protocol, documented in detail in Ref. 26. Here we provide just a quick overview. Every command is formed by two ASCII characters followed by parameters when required. Commands fall in the following four categories: trigger control, execution control, memory access and status request. Trigger control commands select between an internal or an external trigger source. Execution control commands arm the trigger in external mode or start/resume execution in internal mode. There are also two stop commands for ending execution after the next instruction or forcing an immediate stop, respectively. This last command is useful since, as mentioned above, the next instruction could be scheduled after more than 6800 s.

Instructions can be loaded one at time in memory in random order. This is less efficient than grouping many consecutive instructions in a single packet but, on the other hand, it allows arbitrary incremental changes on a program already resident in memory, simplifying multiple executions of programs where only some instructions are changed i.e. for parameter scanning. Due to this choice the command interpreter can not easily determine if a program is complete so a specific command must be sent after loading the last instruction.

Finally a status request command returns to the PC a packet of data specifying the MFSM status (idle, waiting for trigger,

running, stopped at a break point). In the last two cases also the current instruction number is returned.

Presently polling the master module via the status request command is the only way for the PC to determine when a program has terminated due to the USB bus nature (communication can be initiated only by the USB master i.e. the PC). A possible improvement on this behaviour will be discussed in Sec. IV.

As soon as a complete program is loaded, the memory interface starts reading from the SDRAM in bursts of four 16 bits-wide words, so that each burst corresponds to a single instruction, and feeds data to the the input of a dual port FIFO 64 bits-wide with a depth of 512 locations inside the FPGA. The FIFO acts as buffer to provide data to the SFSM even when the SDRAM is busy performing refresh cycles. The combination of FIFO depth and average SDRAM bandwidth guarantees, as shown in Sec. III, that the maximum execution rate of an instruction per MC cycle can be sustained indefinitely.

The SFSM fetches the next instruction from the FIFO just one MC cycle before the current instruction is executed and performs a sequence of operations that, as a first step, involve splitting the instruction in its four components²⁶: the 7 bits address, the 16 bits data, the 36 bits time interval and the 5 control bits. Presently only 3 control bits are used. They are used to mark the last instruction, set a break point and, finally, enable the generation of the strobe pulse. Note that not firing the strobe pulse can be useful both inserting dummy instructions in order to increase the maximum time interval between instructions and to disable the execution of few selected instructions for testing.

The main control program runs on the PC and it is the last software layer. It is responsible for taking a "user friendly" description of the program, usually a timeline of each output, and translating it into a sequence of instructions for one or more DPGs. The concept of "user friendly" is so highly subjective, that has led to a myriad of different solutions. Here, we mention the most recent ones of which we are aware, namely Refs. 14, 15, and 18. We point out that while Ref. 15 uses a graphics library that runs only under the Windows OS, Ref. 14 is written in Python and Ref. 18 is written in C++, and both use a graphics library available for the most common OSs.

We are confident that adding support for our SCH to both the programs mentioned above should be relatively simple however have ported to our DPG two different programs that were previously developed for different hardware, one written in C and the other in Python, following, respectively, the two approaches described above. The source code for both of them is available²⁶.

A useful feature that we included in both codes is the possibility to write a file with a graphical representation of the program regardless of the way in which it was originally generated, in order to have a quick visual check of the experiment: the IEEE standard 1364-2001³⁴ specifies a format for the output of hardware simulations called value change dump (VCD) for which a full-featured open-source viewer is available³³. A VCD file representing a program is a very helpful tool to check what a program does. Fig. 2 shows, as an example,

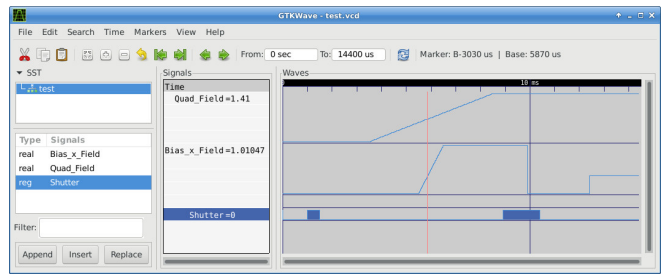


FIG. 2. Screenshot of a VCD file viewer³³. The traces shown are similar to Fig. 2 from Ref. 14, for comparison, and show the timeline of the current in two electromagnets and the status of a shutter. The viewer offers many possibilities to customize the output format and cursors for measuring times, time differences, and the amplitudes of analog signals.

the screenshot of the VCD viewer applied to an experimental sequence involving three signals: the current in two electromagnets and the state of an optical shutter, controlled by a digital output line. The sequence is similar to that reported in Fig. 2 in Ref. 14.

Adopting a control program for an experiment is a choice that ultimately depends on the end-user and will inevitably change over time. We think that a wise choice relies on open-source code that can run on multiple OSs. When designing a master module, the best solution is to use a simple set of commands that can be implemented using as many programming languages as possible, letting the users choose the control program that best suits their needs. As we have seen, our master module communicates through USB packets implementing the commands briefly discussed above, in order to be usable with a broad range of commercial software programs, such as Labview, or programming languages.

III. CHARACTERIZATION / PERFORMANCES

The modular design of the control hardware allows for easy customization of the configuration to meet the specific requirements of the experiment, in terms of the number and type of output signals. Typical instruments that are controlled directly or through specific drivers by such systems include: optical shutters, acousto- and electro-optic modulators, electromagnets, electronic switches, and CCD cameras. Here we would like to focus mainly on the characteristics of our SCH.

Two features of our master module are noteworthy, namely its ability to operate at full speed i.e. to send a command at every MC transition and the possibility to pause and re-trigger using external signals in the same program, at will.

The transmission bandwidth between the SDRAM and the FPGA is sufficient to maintain the peak speed of one instruction per MC cycle, indefinitely at $f_c = 10$ MHz. This is shown in Fig. 3, where a burst of 8 M transitions of a digital output of a DO module, limited only by the SDRAM size, is shown.

Synchronization of the program execution is critical in AMO experiments. The measurement precision can be improved by synchronizing part of the experimental sequence

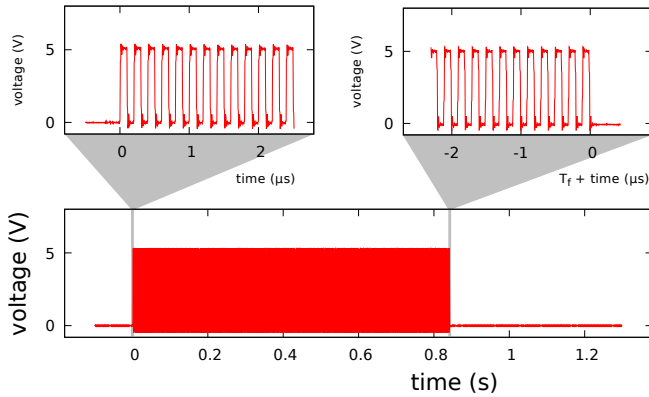


FIG. 3. A digital output line is toggled every 100 ns, i.e. at the full rate given by the 10 MHz signal used to clock the system, for $8\text{ M} = 2^{23}$ times (see 24.). The 5 MHz square wave burst periodicity of the commuting digital output is maintained for the whole sequence, as highlighted by the insets showing the beginning and the end of the program. The time for the final section of the sequence is referred to the falling edge of the last pulse.

with external signals, as discussed in Sec. II A. Moreover, complex setups composed of independently controlled, spatially separated sub-units require a precise synchronization to achieve optimal performances.

Since break points can be inserted in the program at any instruction and the execution resumed via a software command or hardware trigger using a dedicated "Trg" digital input (see Fig. 1), it is simple to synchronize DPGs and relative modules to a master DPG unit. In Fig. 4, we show an example of break points with hardware retriggering. The toggling of a digital output line (red signal) is suspended three times, and each time execution resumes at the first positive edge of the Trg input (blue line), in this case provided by a 20 Hz square wave. Since the output will always be synchronous with the MC and an extra MC cycle is internally used to change state, the worst case latency between the rising edge of Trg and the resuming of execution will be $2/f_c$ or 200 ns in this example. This is, of course, how a SCH is supposed to work and a reduction in latency can only be achieved by increasing f_c .

We have discussed above why, due to the synchronous nature of our hardware, presenting delay and jitter measurements of the DO and AO modules will provide limited information. The delay is dominated by cable length for the DO modules and by DAC settling time for AO modules while jitter is expected to be negligible when compared with $1/f_c$.

It is instead worth showing the use of double-buffered registers in the AD9958 DDS to implement limited strictly synchronous capabilities of the RFO2 module.

Normally a command to the RFO2 module uses the first 10 bits on the data bus to specify an entry in the 1024 elements LUT table. The frequency and amplitude for each channel corresponding to that entry – the phase is not usually changed – are loaded into the the DDS chip by the microcontroller via a serial interface. As mentioned above, this takes about 30 μs per channel. As soon as the DDS registers are loaded,

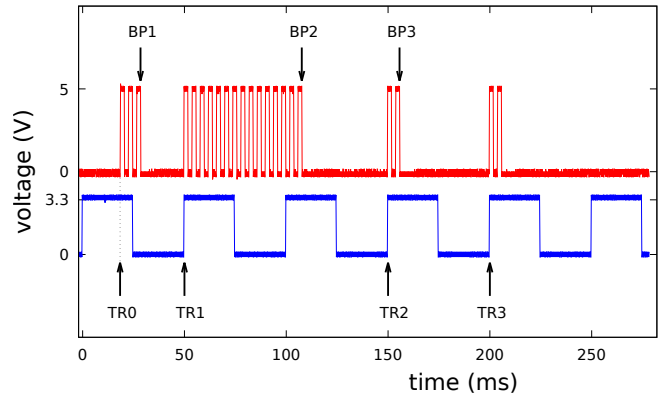


FIG. 4. The sequence in the red trace is triggered via software at a time indicated by TR0 and shows the digital output commuting every 2 ms, hitting 3 break points, after commuting 6, 30, and 4 times, respectively. The three break points are indicated by the labels BP n . The sequence resumes on the positive edges of the blue trace, a square wave at 20 Hz, at the times labelled by TR n . After TR3, the sequence ends with 4 last commutations of the digital line.

the microcontroller pulses a dedicated line actually forcing the new frequency and amplitude to appear at the RF outputs with a delay of few tens of ns. Both the presence of the update pulse and the action of programming the DDS are independently enabled by separate bits on the data bus. New values can be preloaded in the DDS without forcing an update and, later, an update pulse can be applied, without reprogramming the DDS, to change the output in synchronously to a given MC transition.

This is shown in Fig. 5 where the two channels of a RFO2 module initially at 100 MHz, half power (blue) and 50 MHz, full power (red), exchange frequency and amplitude upon receiving an update command from the master module. The pulse is not shown but, for reference, the black trace shows an output line of a DO module generating a pulse with the rising and falling edges one MC cycle before and after, respectively, the update command.

The RF outputs change amplitude and frequency well within 100 ns, meeting the requirements for synchronous operation. Note that the amplitude changes before the frequency. This is in agreement with the DDS datasheet³⁵ where the minimum latencies for amplitude and frequency are specified as 17 and 29 internal clock cycles. Since the DDS is clocked at 400 MHz, the expected latencies are about 42.5 ns and 72.5 ns respectively so amplitudes are expected to change about 30 ns before frequencies. These latencies are limited by the DDS itself therefore compare favorably even with those reported using high speed FPGA to DDS interfaces¹⁶.

The update rate is however limited to about 16 kHz by the time required to pre-programm the DDS registers. Faster rates can be obtained using frequency-shift (amplitude-shift) keying modulation if only one between frequency and amplitude must be changed and no more than 16 different values for a single channel, are required.

The outputs of the RFO2 module share the same clock so

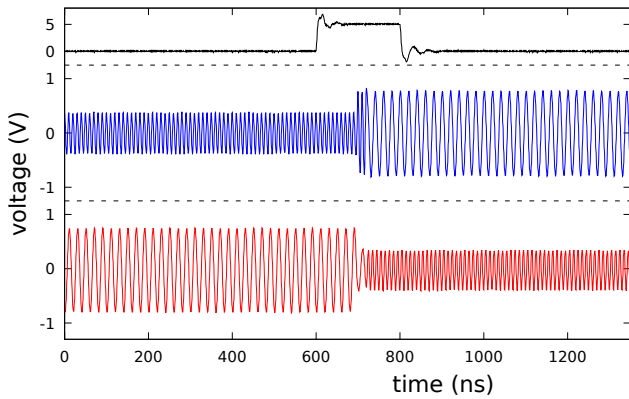


FIG. 5. The RF outputs of a dual channel DDS module initially at 100 MHz, half power (blue trace) and 50 MHz, full power (red trace), exchange frequency and amplitude upon receiving an update command from the master module. For reference a digital line (black trace) generates a 200 ns pulse, centered around the update command. The amplitude change occurring few tens of ns before the phase-continuous frequency change is consistent with the DDS specifications³⁵.

keep a definite phase relation when generating the same frequency. The phase offset $\Delta\phi$, however, depends from the previous history of the channels. It is possible to set $\Delta\phi$ to zero by resetting simultaneously the phase accumulators of both channels inside the DDS chip. Later $\Delta\phi$ can be set to any desired value in the $[0, 2\pi]$ interval with a resolution of 14 bits. The option to set $\Delta\phi = 0$ is not implemented in the current firmware version but can be added, if required.

IV. FURTHER DEVELOPMENTS

The DPG performances can be readily improved by adopting a more powerful FPGA module. This also shows how our approach can tackle obsolescence. The ZTEX 2.13a, from the same manufacturer,²⁸ is essentially pin-compatible but uses more recent and powerful components i.e. a Xilinx Artix 7 FPGA and a 256 MBytes DDR3 SDRAM at 400 MHz, bringing the number of instructions to 64 M and doubling SDRAM peak bandwidth. As a test we have ported, compiled and simulated the Verilog firmware for this module²⁶ but, so far, we have not acquired a physical unit for testing. Note that the ZTEX 2.13a requires a different set of development tools^{36,37}. Using this module pushing f_c to at least 50 MHz should be relatively simple.

Although most experiments will probably need only one DPG module, as we mentioned above, multiple modules can be cascaded and synchronized using break points either for convenience or necessity.

As an example of the first, consider auxiliary modules distributed on 19" racks in different parts of a laboratory. Carrying around long flat cables for distributing the 24 lines of the SCH bus rather than just 2 BNC cables carrying the MC and a DO line from the master DPG rack acting as a trigger would

be both unpractical and possibly prone to noise, especially at high f_c .

In the case of the underground, 150 m long atom-laser antenna MIGA²², a demonstrator we are developing for atom interferometry based gravitational wave detection, multiple DPGs will be instead mandatory. There different atom interferometers, with their electronic subsystems, will be separated by a distance of the order of 100 m so the issue of achieving synchronous operation when the transmission delay is large with respect to the MC period must be addressed.

We have not included in the DPG firmware a syntax for implementing loops which are instead “unrolled” by the PC code before sending a program to the master module. Due to the large amount of memory available and the high communication bandwidth, presently we do not consider this inefficiency as a limiting factor. A more evolved firmware can nevertheless be developed.

By using a distribution amplifier and cables with matched lengths, sufficiently coherent copies of the MC can be distributed among the various subsystem, then the propagation delay between the master DPG and each auxiliary DPG must be determined with an uncertainty better than one MC cycle. Using either BNC cables or optical fibers this corresponds to an uncertainty, in length, that, at $f_c = 10$ MHz, should be small when compared to 20 m. The master DPG then must send a trigger pulse with the correct timing to obtain a distributed SCH.

If simultaneous change of outputs across different DO and AO modules is required, multiple solutions are possible. First, as described above, multiple DPG modules could be used.

As an alternative, with a single DPG, it is possible to reserve a specific address for sending trigger commands. Any DO or AO module decoding both their address and the trigger address could interpret then the content of the data bus as 16 independent trigger lines. This approach requires, however, the design of a new set DO and AO boards where the bus interface is implemented using CPLDs rather than standard TTL chips.

An obvious way to achieve rapid switching of analog outputs is using auxiliary modules containing some 2^n -to-one analog multiplexers, where 2^n analog outputs and n digital outputs are required for a single, fast switching, analog output among 2^n preset values. The cost in term of hardware resources is compensated by a switching time limited not by the DAC but by the multiplexer.

As we mentioned before, a DPG module with only a USB interface has the disadvantage that it cannot initiate communication. Moreover including an Ethernet interface to our SCH will help integration with other systems. Both issues can be solved by adding a simple auxiliary credit-card size computer with USB and Ethernet interfaces and digital input signals capable of generating interrupts, acting as bridge and, possibly, as protocol translator between the DPG and other hardware. The DPG could use one of the DO lines to fire an interrupt in the auxiliary computer, which will forward a service request to the main PC via Ethernet. An obvious application could be notify program termination instead of relying on polling.

Even without hardware changes there is room for soft-

ware improvements that, mostly, could improve reliability. A simple example is given by the handling of break points. Presently the software in the PC can easily determine, by polling, how long the DPG has been waiting at a break point. It could be useful to set a sensible timeout policy to resume execution or abort the program and set the experiment in a safe condition.

V. CONCLUSIONS

We have presented a control hardware developed for experiments in AMO physics; it is broadly applicable to experimental science. The system provides up to hundreds of digital, analog, and RF signals controlled with a time resolution of 100 ns, with a wealth of possible configurations. The program execution can be synchronized with external events at multiple times in the same sequence. Several improvements can be easily adopted to the system: the time resolution could be increased by a factor of 5 to 20 ns by changing the main clock frequency and with simple modifications of the firmware; the maximum number of instructions in a program could be increased by a factor of 4 by adopting a different FPGA board. The modular nature of the system makes it easy to adapt parts of it, especially the low-cost DPG module, to other applications and make it more resilient against inevitable obsolescence. In general, the system could be engineered to be compatible with portable or space applications, in terms of weight, volume, and power consumption.

ACKNOWLEDGMENTS

This work has been partly founded by the “Agence Nationale pour la Recherche” (grant EOSBECMR # ANR-18-CE91-0003-01, grant ALCALINF # ANR-16-CE30-0002-01, grant MIGA # ANR-11-EQPX-0028), Laser and Photonics in Aquitaine (grant OE-TWC), Horizon 2020 QuantERA ERANET (grant TAIOL # ANR-18-QUAN-00L5-02), and the Aquitaine Region (grants IASIG-3D and USOFF). M.C. acknowledges support by DSTL-DGA. M.P. would like to thank for useful discussions and constant support M. De Pas, M. Giuntini and A. Montori at the electronic workshop of the European Laboratory for Nonlinear Spectroscopy (LENS), Firenze.

¹Virtual Instruments Software Architecture (VISA): www.ivifoundation.org/specifications. Both commercial (www.ni.com/visa) and public domain (github.com/hgrecco/pyvisa, limited to GPIB, USB and RS-232 so far) implementations are available. For the Linux OS an effort to a unified approach to data acquisition is represented by Comedi (comedi.org). We mention commercial products at the sole purpose of identification for helping the reader to reproduce our setup. We do not endorse any specific product. Products with similar or even better performances might be available.

²Tango: www.tango-controls.org.

³Experimental Physics and Industrial Control System (EPICS): epics-controls.org.

⁴As an example, National Instruments offers a real-time module for the Labview programming environment: www.ni.com/en-us/shop/select/labview-real-time-module.

⁵Two real-time open source extensions for Linux are RTAI (www.rtai.org) and Xenomai (xenomai.org).

⁶G. Rosi, F. Sorrentino, L. Cacciapuoti, M. Prevedelli, and G. M. Tino, “Precision measurement of the Newtonian gravitational constant using cold atoms,” *Nature* **510**, 518 (2014).

⁷See, e.g., the National Instruments series of PCI boards (www.ni.com/en-us/shop/select/digital-waveform-device) or the PulseBlaster series at Spin Core (spincore.com/products/#pulsegeneration).

⁸R. Hořák and M. Ježek, “Arbitrary digital pulse sequence generator with delay-loop timing,” *Rev. Sci. Instrum.* **89**, 055103 (2018).

⁹B. S. Malek, Z. Pagel, X. Wu, and H. Müller, “Embedded control system for mobile atom interferometers,” *Rev. Sci. Instrum.* **90**, 073103 (2019).

¹⁰L. Pezzè, A. Smerzi, M. K. Oberthaler, R. Schmied, and P. Treutlein, “Quantum metrology with nonclassical states of atomic ensembles,” *Rev. Mod. Phys.* **90**, 035005 (2018).

¹¹A. D. Ludlow, M. M. Boyd, J. Ye, E. Peik, and P. Schmidt, “Optical atomic clocks,” *Rev. Mod. Phys.* **87**, 637–701 (2015).

¹²I. Georgescu, S. Ashhab, and F. Nori, “Quantum simulation,” *Rev. Mod. Phys.* **86**, 153–185 (2014).

¹³P. E. Gaskell, J. J. Thorn, S. Alba, and D. A. Steck, “An open-source, extensible system for laboratory timing and control,” *Rev. Sci. Instrum.* **80**, 115103 (2009).

¹⁴P. T. Starkey, C. J. Billington, S. P. Johnstone, M. Jasperse, K. Helmerston, L. D. Turner, and R. P. Anderson, “A scripted control system for autonomous hardware-timed experiments,” *Rev. Sci. Instrum.* **84**, 085111 (2013).

¹⁵A. Keshet and W. Ketterle, “A distributed, graphical user interface based, computer control system for atomic physics experiments,” *Rev. Sci. Instrum.* **84**, 015105 (2013).

¹⁶T. Pruttivarasin and H. Katori, “Compact field programmable gate array-based pulse-sequencer and radio-frequency generator for experiments with trapped atoms,” *Rev. Sci. Instrum.* **86**, 115106 (2015).

¹⁷S. Bourdeauducq *et al.*, “m-labs/artiq: 4.0,” (2018).

¹⁸E. Perego, M. Pomponio, A. Detti, L. Duca, C. Sias, and C. E. Calosso, “A scalable hardware and software control apparatus for experiments with hybrid quantum systems,” *Rev. Sci. Instrum.* **89**, 113116 (2018).

¹⁹S. Donnellan, I. R. Hill, W. Bowden, and R. Hobson, “A scalable arbitrary waveform generator for atomic physics experiments based on field-programmable gate array technology,” *Rev. Sci. Instrum.* **90**, 043101 (2019).

²⁰Group of F. Schreck (Amsterdam) <http://www.strontiumbec.com/Control/Control.html>.

²¹Electronic shop at LENS (Florence) <http://ew.lens.unifi.it/>.

²²B. Canuel, A. Bertoldi, L. Amand, E. P. di Borgo, T. Chantrait, C. Danquigny, M. D. Álvarez, B. Fang, A. Freise, R. Geiger, J. Gillot, S. Henry, J. Hinderer, D. Holleville, J. Junca, G. Lefèvre, M. Merzougui, N. Mielec, T. Monfret, S. Pelisson, M. Prevedelli, S. Reynaud, I. Riou, Y. Rogister, S. Rosat, E. Cormier, A. Landragin, W. Chaibi, S. Gaffet, and P. Bouyer, “Exploring gravity with the MIGA large scale atom interferometer,” *Sci. Rep.* **8**, 14064 (2018).

²³D. S. Naik, G. Kuyumjyan, D. Pandey, P. Bouyer, and A. Bertoldi, “Bose–Einstein condensate array in a malleable optical trap formed in a traveling wave cavity,” *Quantum Sci. Technol.* **3**, 045009 (2018).

²⁴To avoid confusion, we will always use $M = 2^{20}$ and never $M = 10^6$ when referring to memory size and number of instructions.

²⁵We make a distinction between a master module and an intelligent one since in a distributed architecture many auxiliary modules are intelligent.

²⁶M. Prevedelli *et al.*, “Yet another control system for AMO physics,” (2019).

²⁷F. Schreck, *Mixtures of ultracold gases: Fermi sea and Bose-Einstein condensate of Lithium isotopes*, Ph.D. thesis, Univ. Pierre et Marie Curie - Paris VI (2002).

²⁸ZTEX FPGA Board with Open Source SDK, Models 2.04b and 2.13a www.ztex.de.

²⁹STEMlab 125-14, formerly Red Pitaya, redpitaya.com.

³⁰Available at sdcc.sourceforge.net.

³¹Available at www.xilinx.com/products/design-tools/ise-design-suite/ise-webpack.html.

³²See opencores.org.

³³See gtkwave.sourceforge.net.

³⁴“IEEE Standard Verilog Hardware Description Language,” IEEE Std 1364-2001, 1–792 (2001).

³⁵Available at www.analog.com/media/en/technical-documentation/data-sheets/AD9958.pdf.

³⁶Available at www.cypress.com/documentation/software-and-drivers/ez-usb-fx3-software-development-kit.

³⁷Available at www.xilinx.com/products/design-tools/vivado/vivado-webpack.html.